

## Microstructure characteristics and mechanical properties of the interface layer of coated steel insert-aluminum bimetals

Maryam Salimi

*Department of Mechanical Engineering, Shahid Rajaei Teacher Training University (SRTTU), Tehran 1678815811, Iran*

Medhi Malekan<sup>a)</sup>

*School of Metallurgy and Materials Engineering, College of Engineering, University of Tehran, Tehran 1417614418, Iran*

Bahram Nami

*Department of Mechanical Engineering, Shahid Rajaei Teacher Training University (SRTTU), Tehran 1678815811, Iran*

Hamed Hoseiny

*Corrosion Research Group, Research Institute of Petroleum Industry (RIPI), Tehran 1485733111, Iran*

(Received 29 October 2016; accepted 11 January 2017)

The effect of aluminizing and Cu electroplating of the steel insert in fabrication of Al-matrix bimetal on the microstructure and mechanical properties of the interface layer was investigated. Compound casting process was used to fabricate Al-matrix bimetals reinforced with coated steel insert. The microstructures at the interface region were studied using light optical and scanning electron microscopes and energy dispersive X-ray spectroscopy. The interfacial shear strengths of the fabricated bimetals were compared using push-out test. The results showed that electroplating with copper and aluminizing of steel insert in aluminum matrix led to significant improvement of metallurgical bonding between the steel and aluminum cast matrix. Cu-coated insert contained a thicker and uniform reaction layer formed at the interface between the steel insert and aluminum matrix compared to aluminized coated insert. The results of push-out tests indicated higher interfacial shear strength for the bimetal with Cu-coated insert despite possessing a larger thickness.

### I. INTRODUCTION

The use of light materials has attracted considerable interest in transportation industry to enhance the engine performance and reduce fuel consumption. This cannot be achieved by only use of light metals but often requires tailor-made materials which can preserve other properties such as strength, toughness, etc. In this respect, the aluminum alloys are used extensively in transportation industry due to their low weight and good corrosion resistance compared to steel. However, to improve the mechanical strength of the aluminum components they can be reinforced by a stronger metal insert such as steel alloys especially at the load-bearing regions. These materials which are made of a lighter matrix (such as Al) and an insert with higher strength (such as steel) are called bimetal.<sup>1,2</sup> One of the principal methods to fabricate the bimetals is compound casting. In compound casting two metallic metals, one solid and one in liquid state, are combined,<sup>3,4</sup> in a way that a diffusion zone between the

two materials is created, hence, a continuous metallic transition from one metal to the other is formed.<sup>4,5</sup>

Difference in chemical and physical properties of Al and Fe as well as their limited solubility at the contact temperature are of the main challenges in compound casting of these two metals.<sup>6</sup> In addition, the formation of intermetallic phases at the reaction zone is the other difficulty one may face in combining steel and Al alloys, since these intermetallics are substantially hard and brittle and are detrimental to the mechanical properties of the fabricated bimetal.<sup>7,8</sup>

To improve the performance of Al-matrix/steel insert bimetal, the thickness and composition of the reaction layer should be controlled. Coating the steel to act as an intermediate layer is an effective method to improve the bonding between the Al matrix and steel insert, hence, is the focus of this study. Recently, some attempts are done to control the thickness and composition of the reaction layer by applying different coatings on the steel insert.<sup>6,9,10</sup>

A357 aluminum alloy has been used to hot-dip aluminizing as coat of insert due to presence of Si and Mg in Al bath. 2.5% Si content in aluminum alloy lead to diminish thickness of intermetallic layer.<sup>11–13</sup> Synergic effects of Si and Mg in A357 melt brings about the minimum layer thickness in comparison to the other

Contributing Editor: Jürgen Eckert

<sup>a)</sup>Address all correspondence to this author.

e-mail: mmalekan@ut.ac.ir

DOI: 10.1557/jmr.2017.32

aluminum alloys.<sup>14</sup> The presence of silicon in Al alloy alters the microstructure of the aluminide layer and transforms the Fe–Al intermetallic compounds into Fe–Al–Si intermetallic compounds.<sup>11,12,15</sup> Five types of phases ( $\text{AlFe}_3$ ,  $\text{Al}_2\text{Fe}$ ,  $\text{Fe}_2\text{Al}_5$ ,  $\text{FeAl}$  and  $\text{FeAl}_3$ ) may be formed in Fe–Al binary system.<sup>16</sup> Although the presence of Si in Fe–Al system makes the study of the intermetallic complicated. Ten types of intermetallic phases ( $\tau_1$ – $\tau_{10}$ ) have been discovered in Fe–Al–Si system.<sup>17–20</sup> There is little information in the published literature on the effect of Cu coating on steel insert as an intermediate material between Fe and Al. It is reported that copper decreases the activity coefficient of aluminum at the interface and consequently decreases the thickness of the reaction layer.<sup>21</sup> In addition, presence of copper in aluminum alloy improves wettability with the steel substrate leading to decrease in the reaction layer thickness.<sup>22</sup>

In the present study, the microstructure and mechanical properties of the interface between Cu/aluminide-coated insert and aluminum matrix were investigated.

## II. EXPERIMENTAL PROCEDURE

### A. Compound casting process

Compound casting process was used to fabricate steel insert in aluminum matrix bimetal. The cylindrical inserts were made of Mo40 steel with internal diameter 10 mm, external diameter 20 mm, and length of 30 mm. Chemical compositions of the steel inserts were Fe–0.372C–0.269Si–0.845Mn–0.0088P–0.016S–0.532Cr–0.224Mo–0.503Ni (wt%). Surface preparation of steel inserts was carried out by polishing to 1000 grit to remove surface oxides followed by ultrasonic cleaning in acetone. Subsequently, two different coatings (aluminide and copper) were applied on the surface of the steel inserts, as explained in the following section. After applying the coatings, the inserts were cleaned with acetone and placed in a cylindrical  $\text{CO}_2$  sand mold with internal diameter of 60 and 60 mm length. 3 Kg of 1035 aluminum alloy (Al–0.097Si–0.061Fe–0.0135Cu–0.006Mn–0.003Mg–0.006Zn) was melted in a resistance furnace using a graphite crucible and poured into the mold at 780 °C.

### B. Coatings

Hot dipping process in A357 aluminum alloy melt was used to apply the aluminide coating on the surface of the steel inserts. In this respect, a commercial A357 aluminum alloy was melted in a graphite crucible with 1 Kg capacity. The chemical composition of the molten aluminum alloy was Al–7.2 Si–0.6 Mg–0.15 Ti–0.05 Be (%wt). The steel inserts were preheated to 200 °C and then immersed into Al melt at 720 °C. After 20 min immersion, the inserts were pulled out of the aluminum bath and cooled to room temperature in the air. The

aluminum oxide layer that was formed at the exterior surface of the inserts was removed by grinding and polishing to 1000 grit.

For coating of the inserts by copper, electroplating process was used. The inserts were ultrasonically cleaned in acetone bath and rinsed with distilled water. The electroplating bath was prepared by adding Cu-sulfate (200 g/L) and sulfuric acid (80 g/L) into 1 L of deionized  $\text{H}_2\text{O}$ . Subsequently, the inserts were placed in bath with 6–8  $\text{A}/\text{dm}^2$  current density for 15 min at 40 °C. At the end of this process, a copper coating with 12  $\mu\text{m}$  thickness was deposited on insert surface.

The thicknesses of the reaction layers of the coatings were measured using light optical microscope (LOM) and scanning electron microscope (SEM). 10 measurements were done for each coating and the average value along with the variations was reported.

### C. Microstructure characterization

The interfaces of the fabricated bimetal specimens, i.e., aluminide-coated insert–aluminum matrix (hereafter AlCoat), and Cu-coated insert–aluminum matrix (hereafter CuCoat), beside the aluminized steel insert (before Al casting) were characterized by means of a LOM and a MIRA3 TESCAN SEM (TESCAN, Brno, Czech Republic) equipped with a field emission gun and energy dispersive spectroscopy (EDS) detector. The metallography specimens were cut from the middle of the fabricated bimetal specimens, perpendicular to the main axis using wire cut. The specimens were prepared by grinding to 2000 grit and final polishing with 0.05  $\mu\text{m}$  alumina suspension.

### D. Push-out test

To measure the shear strength of the interfacial regions, push-out test was performed based on ASTM F1820<sup>9,23,24</sup> using a Gotech AI-7000 LA10 testing machine (Gotech Testing Machines Inc., Taichung City, Taiwan). Push-out test is a standard test procedure to measure the attachment strength between the modular acetabular shell and liner. The test equipment is shown schematically in Fig. 1. For each coated insert, three tests were performed. Test specimens were prepared by round cut at the middle of steel insert–aluminum matrix bimetal with 10 mm height. The samples were placed on a platform with a circular support hole (24 mm in diameter) which supports the shell (here, aluminum matrix) and the insert was pushed under an axial force using a flat-bottom steel cylinder (18 mm in diameter) until a complete detachment between the insert and coating occurred. The displacement speed was constant at 5 mm/min. The testing machine provides the results as load-displacement curves. The shear strength was calculated according to

$$\tau = \frac{L}{P(t-d)} \quad (1)$$

where  $L$  is the peak load,  $P$  is the perimeter of the insert,  $t$  is the insert height, and  $d$  is measured insert displacement at maximum load excluding elastic displacement.

### III. RESULTS AND DISCUSSION

#### A. Microstructure of aluminide-coated insert and bimetal with Al coating (AlCoat)

Figure 2 shows an optical micrograph of aluminide coating on the steel insert. The coating consisted of an outer layer and a reaction layer adjacent to the steel insert. The outer layer includes Al( $\alpha$ ) phase with a dendritic structure, eutectic Al–Si phase, and  $\alpha$ -Al<sub>3</sub>Fe<sub>2</sub>Si Chinese script phase distributed in the interdendritic regions. Formation of reaction layer at the interface is a result of interdiffusion of Al–Si alloy melt and steel insert. Si content of the molten aluminum affects the thickness, morphology, and composition of the reaction layer.<sup>25</sup> It seems that Si alters the reaction path between aluminum

and steel in the early stages of the contact,<sup>26</sup> thus reduces the reaction layer thickness and changes the morphology of the interface between reaction layer and substrate. In addition, it has been reported that Si is an impurity element in molten aluminum which decreases the activity coefficient of Al atoms in steel, leading to reduction in the thickness of the reaction layer at the interface.<sup>21</sup>

Macroscopic image and optical micrograph of the cross section of AlCoat bimetal are illustrated in Fig. 3. The thickness of the reaction layer formed in the aluminide-coated insert–aluminum matrix interface in this specimen is about  $21 \pm 2 \mu\text{m}$ . The thickness of the reaction layer was almost uniform along the length of coated sample as can be determined from the variations calculated as standard deviation. The comparison of the micrographs of Al-coated insert and the AlCoat bimetal shows that the Al coating had been dissolved in pure aluminum melt during casting.

Figure 4 shows SEM micrographs of aluminide-coated insert at reaction layer [Fig. 4(a)] and the interface layer of AlCoat bimetal [Fig. 4(b)]. The thickness of the reaction layers in both of the specimens is almost the same but some differences can be seen in phases and their morphology, e.g., the interface of the reaction layer in AlCoat bimetal has more rough morphology.

Chemical composition of each region in the reaction layer was evaluated by EDS and the results are presented in Tables I and II along with the suggested phases. According to phase constitution analysis of reaction layer in Fig. 4(a), adjacent phases to the steel insert are Fe<sub>2</sub>Al<sub>5</sub> phase (region B) and then FeAl<sub>3</sub> phase (region D) with dispersed Si-rich phase of  $\tau_1$ -Al<sub>2</sub>Fe<sub>3</sub>Si<sub>3</sub> (C). Chemical composition of the reaction layer adjacent to outer layer corresponds to  $\tau_5$ -Al<sub>7</sub>Fe<sub>2</sub>Si phase (region E) along with  $\tau_6$ -Al<sub>9</sub>Fe<sub>2</sub>Si<sub>2</sub> phase (F). The dominant mechanism for formation of the reaction layer was interdiffusion between steel insert and molten Al–Si alloy during hot-dip

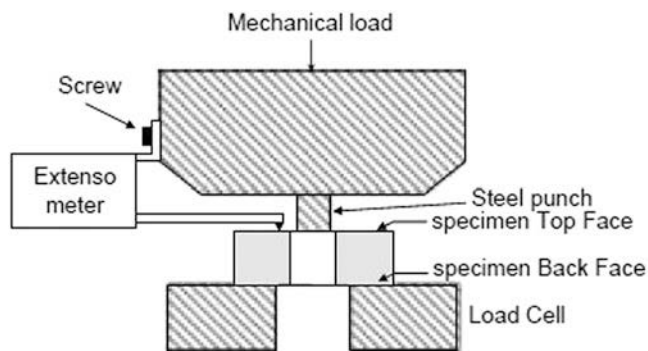


FIG. 1. Schematic illustration of the push-out test machine.

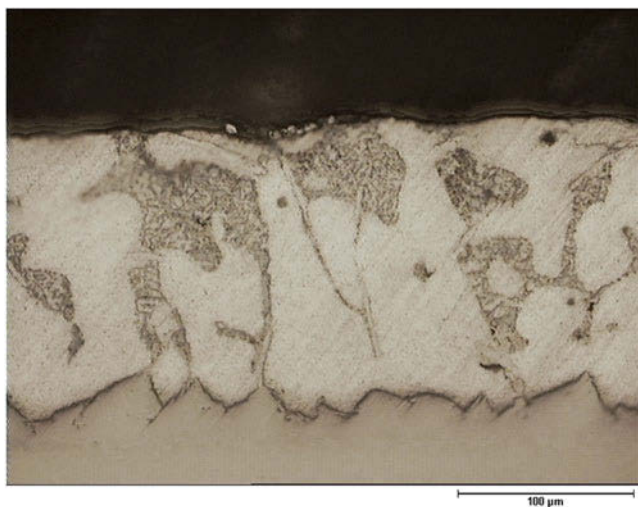


FIG. 2. Optical micrograph of the aluminide layer formed on the steel insert before casting.

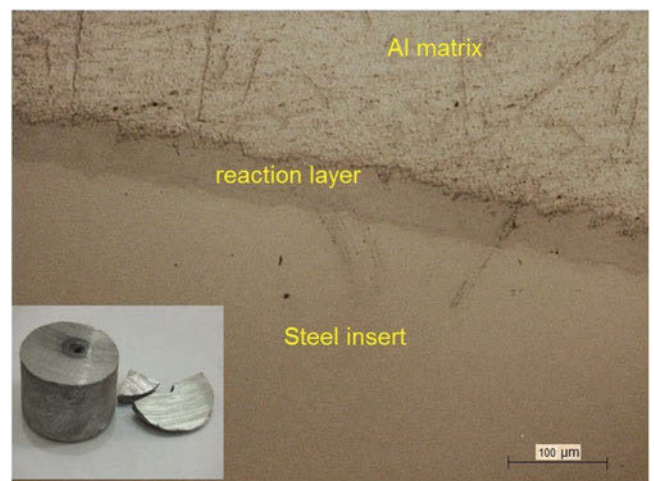


FIG. 3. Macroscopic image and optical micrograph of the aluminized insert–aluminum matrix interface.

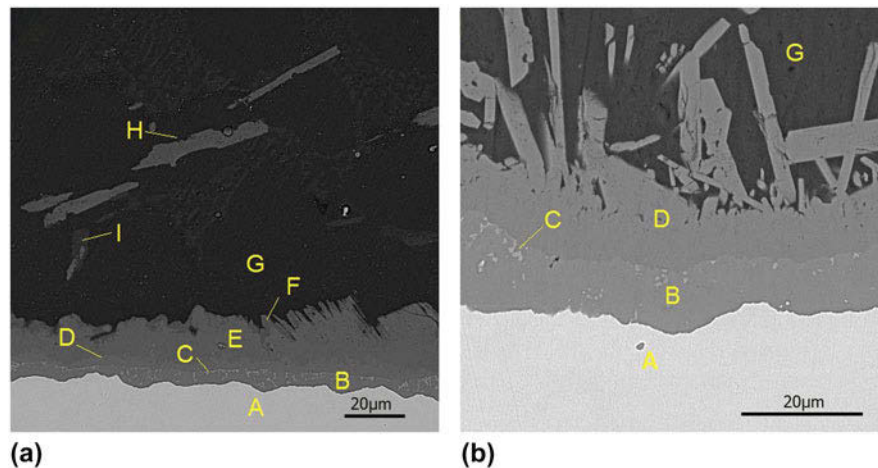


FIG. 4. SEM micrographs showing the microstructure at the interface, (a) aluminide-coated insert at the reaction layer, (b) aluminide-coated insert–aluminum matrix bimetal.

TABLE I. EDS chemical analysis of phases formed in aluminide-coated insert [shown in Fig. 4(a)] and the suggested phases.

Region (as shown in Fig. 4a)	Fe (wt%)	Al (wt%)	Si (wt%)	Mg (wt%)	Suggested phase
A	96.57	0.58	0.51	...	Steel insert
B	42.35	52.68	3.06	...	$\text{Al}_3\text{Fe}_2$
C	48.04	35.07	14.37	...	$\tau_1\text{-Al}_2\text{Fe}_3\text{Si}_3$
D	54.03	37.32	6.21	...	$\text{FeAl}_3$
E	31.07	57.38	9.14	...	$\tau_5\text{-Al}_7\text{Fe}_2\text{Si}$
F	23.6	57.39	16.69	...	$\tau_6\text{-Al}_9\text{Fe}_2\text{Si}_2$
G	0.32	89.86	2.32	...	Al–Si top-coat
H	7.38	49.46	24.8	14.61	$\text{Al}_8\text{Mg}_3\text{FeSi}_6$
I	23.59	58.39	15.42	...	$\tau_6\text{-Al}_9\text{Fe}_2\text{Si}_2$

TABLE II. EDS chemical analysis of phases formed in the interface layer of AlCoat bimetal [shown in Fig. 4(b)] and the suggested phases.

Region [as shown in Fig. 4(b)]	Fe (wt%)	Al (wt%)	Si (wt%)	Mg (wt%)	Suggested phase
A	94.15	0.15	0.20	...	Steel insert
B	41.53	52.5	1.78	...	$\text{Al}_3\text{Fe}_2$
C	46.6	39.00	10.21	...	$\tau_1\text{-Al}_2\text{Fe}_3\text{Si}_3$
D	37.04	57.51	1.54	...	$\text{FeAl}_3$
G	0.14	90.16	1.81	...	Al matrix

process. Phase I, in the outer layer, with the plate-shape morphology and composition of Al–23.6% Fe–16.7% Si (wt%) was identified as  $\tau_6\text{-Al}_9\text{Fe}_2\text{Si}_2$  phase. The other phase formed in the outer layer (phase H) was identified as  $\text{Al}_8\text{Mg}_3\text{FeSi}_6$  phase according to its chemical composition determined by EDS.<sup>27,28</sup> It is worth to mention that no Mg was observed in the reaction layer. Mg usually is piled up at the interface between the reaction layer and the melt which can retard the growth of reactive phase.<sup>14</sup> The results (phase identification) described above are generally in good agreement with the most of the previous findings.<sup>27–30</sup>

Casting of pure aluminum melt on aluminide-coated insert caused some changes in the reaction layer. Irregularity of the interface between reaction layer

and aluminum matrix [Fig. 4(b)] was resulted from the detachment of the intermetallic phases from the insert surface due to contact with the turbulent aluminum melt. High temperature of the melt and diffusion are the main parameters assisting the variations in the phases.  $\tau_5$  and  $\tau_6$  phases in the reaction layer were replaced by growth of the Fe–Al intermetallic phases.<sup>29</sup> The reaction layer in this bimetal specimen consisted of only 3 phases after casting of aluminum. The entire reaction layer turned into 2 continuous intermetallic layers, i.e.,  $\text{Fe}_2\text{Al}_5$  and  $\text{FeAl}_3$  phases which contained dispersed phase  $\tau_1$ . By casting aluminum on the coated insert, the silicon content and dispersed phase  $\tau_1$  were reduced in the reaction layer. Some amounts of Si were dissolved in the phases  $\text{Fe}_2\text{Al}_5$  and  $\text{FeAl}_3$  as observed by EDS.



The presence of iron in liquid aluminum leads to formation of isolated needle-shaped intermetallic phases in aluminum matrix.<sup>1</sup> It can be noted that dissolution of iron in aluminum does not have the conventional mode of diffusion of iron atoms and their subsequent dissolution in molten aluminum. The breakage of intermetallic phase and floating of the broken blocks in the molten aluminum provides the iron content required for the formation of intermetallic needles within aluminum. The detaching and spalling of  $\text{FeAl}_3$  phase in reaction layer showed that this phase acts as a source of iron for the formation of needle-shaped intermetallic particles.

The results showed that the number of phases formed in the reaction layer decreased after aluminum casting, but the thickness of intermetallic layer did not change. Indeed, during casting of aluminum melt on aluminide-coated insert, the intermetallic layer at the interface inhibited the interdiffusion of Fe and Al elements.

Figure 5(a) shows the result of the EDS line scan on the AlCoat bimetal over the steel insert-aluminum matrix

interface. A typical EDS map of the Al, Fe, O, and Si elements is shown in Fig. 5(b) which corresponds to the SEM micrograph of Fig. 4(b).

Comparing the distribution maps of Al, Fe, and Si elements reveals that contrary to the Al, concentration of Fe decreases with distance from the steel insert. It can be also observed that the concentration of Si in reaction layer is less than that of aluminum matrix adjacent to the reaction layer, due to the migration of Si element at high temperatures.

## B. Microstructure of Cu-coated (CuCoat) bimetal

Figure 6 shows an optical micrograph of the cross section of CuCoat bimetal at the around the interface. It can be seen that a relatively uniform interface formed due to the suitable contact between coated steel insert and aluminum melt. The coarse intermetallic phases are clearly visible just above the interface in the aluminum matrix. Thickness of the reaction layer in this specimen is

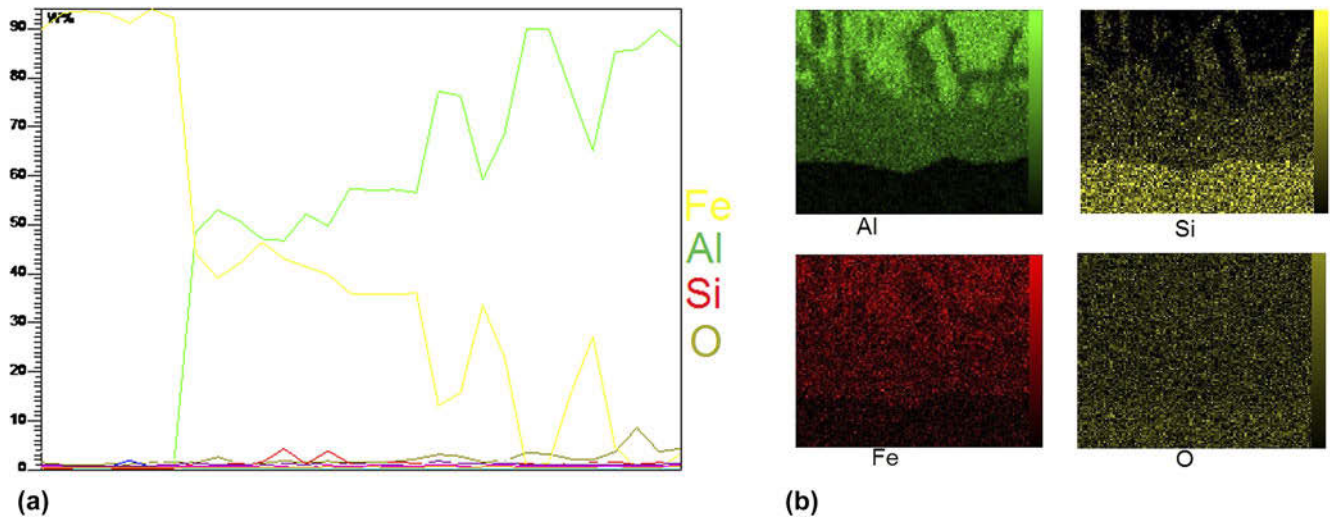


FIG. 5. The results of EDS, (a) line scan, (b) elemental map analyses over the interface in AlCoat bimetal specimen.

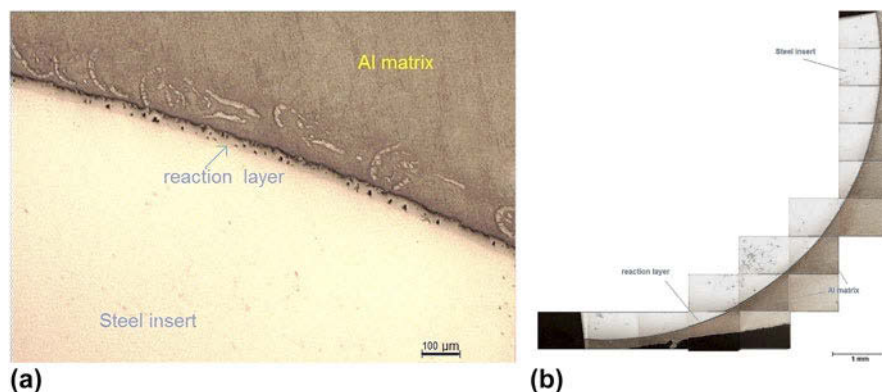


FIG. 6. Optical micrograph of the cross section of CuCoat bimetal at the steel/Al interface, (a) high magnification, (b) low magnification panoramic image.

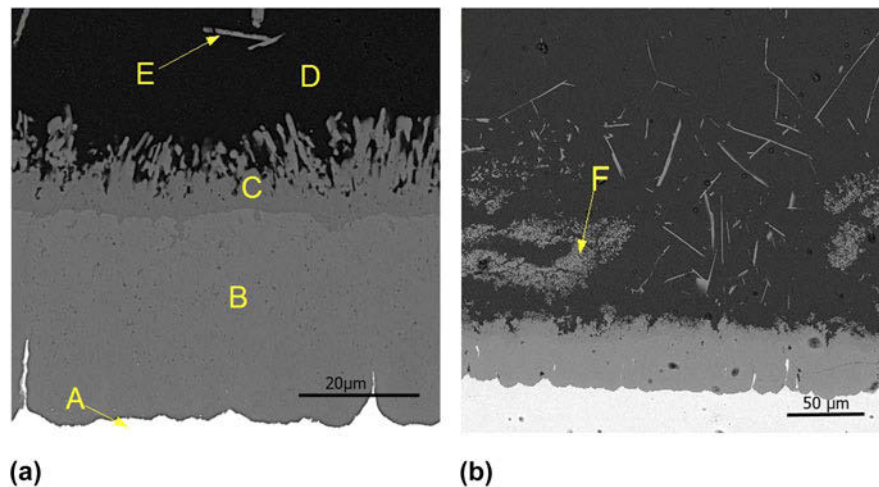


FIG. 7. (a) and (b) SEM micrographs showing the interface between Cu-coated insert and aluminum matrix in CuCoat bimetal specimen.

about  $39 \pm 2 \mu\text{m}$ . The thickness of the reaction layer was almost uniform along the length of coated sample as can be determined from the variations calculated as standard deviation. The thickness of the reaction layer in CuCoat bimetal is larger than that of AlCoat bimetal specimen. It seems that electroplating the steel insert by copper could effectively improve the bonding between steel insert and aluminum matrix.

Two possible mechanisms for the influence of Cu coating as an intermediate layer on the steel insert are suggested. Firstly, Cu coating on steel insert prevents the contact between the aluminum melt and steel insert, consequently the formation of intermetallic phases. Secondly, Cu element likely decreases the activity coefficient of aluminum at the interface,<sup>21,22</sup> hence, decreases the thickness of the reaction layer compared to when the steel insert is in direct contact with aluminum.

It seems that aluminizing of steel insert has more significant effect on reducing the reaction layer thickness at the steel–aluminum interface; however, the coatings influence the reaction layer with different mechanisms. In the case of AlCoat bimetal, due to presence of intermetallic phases at the reaction layer, coating of steel insert was not melted over pouring the aluminum melt; hence, molten aluminum was not in direct contact with steel substrate and less thickness of reaction layer at the interface was obtained. On the other hand, Cu was melted by molten metal, and the direct contact between the steel substrate and aluminum resulted in thicker reaction layer.

Figure 7 shows SEM micrographs of CuCoat bimetal. It can be observed that the reaction layer between steel and aluminum consists of 2 continuous intermetallic layers (B and C) and some intermetallic phases dispersed within the aluminum matrix (E and F). Table III presents EDS analyses of the intermetallic phases formed between Cu-coated insert and aluminum matrix along with

TABLE III. EDS chemical analysis of phases formed in the interface layer of CuCoat bimetal [shown in Figs. 7(a) and 7(b)] and the suggested phase.

Region	Fe (wt%)	Al (wt%)	Suggested phase
A	97.78	0.19	Steel insert
B	41.33	55.47	$\text{Al}_5\text{Fe}_2$
C	36.41	60.46	$\text{FeAl}_3$
D	0.34	90.97	Aluminum matrix
E	33.14	63.77	$\text{FeAl}_3$
F	33.74	63.31	$\text{FeAl}_3$ or $\text{FeAl}_6$

suggested formulas for each phase. As can be seen,  $\text{Fe}_2\text{Al}_5$  is the major constituent phase instead of  $\text{FeAl}_3$  in contradiction with thermodynamic principle. Kinetics of reaction at the interface may result in formation of  $\text{Fe}_2\text{Al}_5$  as the major phase in the reaction layer.<sup>31</sup> EDS line scan results over the interface is shown in Fig. 8(a). The sudden decrease in Al and increase in Fe concentrations at the right side of the line scan spectrum is probably due to the presence of an intermetallic phase in the Al matrix. Elemental maps of Al, Fe, Si, and Cu are shown in Fig. 8(b) which is correspondent to the SEM micrograph shown in Fig. 7(a). The results of EDS analyses showed that no significant amount of Cu existed at the diffusion layer between the steel insert and Al matrix which is probably due to melting of Cu coating and dissolving in the turbulent aluminum melt.

The chemical composition of the layer adjacent to the steel insert within the reaction layer corresponds to  $\text{Fe}_2\text{Al}_5$  phase and the one adjacent to the aluminum matrix matches  $\text{FeAl}_3$  phase. It has been reported that  $\text{Fe}_2\text{Al}_5$  and  $\text{FeAl}_3$  phases form when molten aluminum is in contact with solid Fe.<sup>25,31,32</sup> Therefore, the Cu coating can only influence the thickness of the reaction layer but not the type of intermetallic phases formed in this layer. Figure 7 shows two different morphologies for the

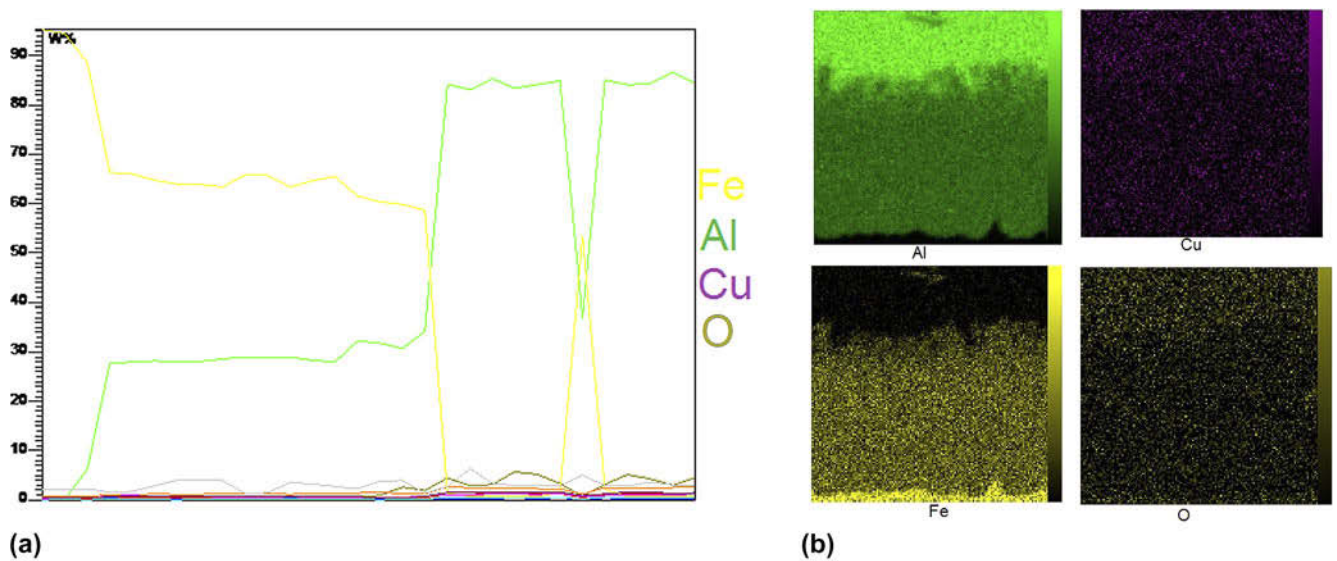
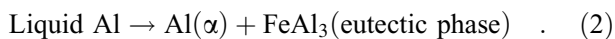


FIG. 8. The results of EDS, (a) line scan, (b) elemental map analyses over the interface in CuCoat bimetal specimen.

intermetallic phases within aluminum matrix (E and F phases), i.e., fine eutectic-shaped and isolated needle-like. The reaction occurring in liquid aluminum containing Fe during solidification is as the following<sup>33</sup>:



FeAl<sub>3</sub> eutectic phase contains fine particles which represent those areas that were solidified at the latest stages of solidification. Backerud<sup>34</sup> reported that non-equilibrium FeAl<sub>6</sub> phase forms instead of FeAl<sub>3</sub> in eutectic reaction. The constituents of the eutectic phase in the Al matrix in CuCoat bimetal could not be detected by EDS due to their small size similar to a previous work.

### C. Push-out test

The typical push-out load–displacement curves of aluminum matrix reinforced with two different coated steel inserts are shown in Fig. 9. The maximum interface shear strength for each insert condition was calculated based on the obtained results. The shear strength value of AlCoat and CuCoat bimetals are obtained as  $23 \pm 2$  MPa and  $31 \pm 3$  MPa, respectively. The shear strength value of AlCoat bimetal is in agreement with the findings of Aguado et al.<sup>9</sup>

In both curves, a linear increase in load is observed at the earlier stage of the test. The rupture of interface occurred at the point of peak load, and subsequently the load began to decrease. Generally, resistance to displacement is caused by sliding friction at the interface of steel insert–aluminum matrix. The intermetallic phases formed in the reaction layer (Fe<sub>2</sub>Al<sub>5</sub> and FeAl<sub>3</sub> phases) are detrimental to the interfacial bonding strength.<sup>6,35</sup> The microhardness indentation showed that both layers

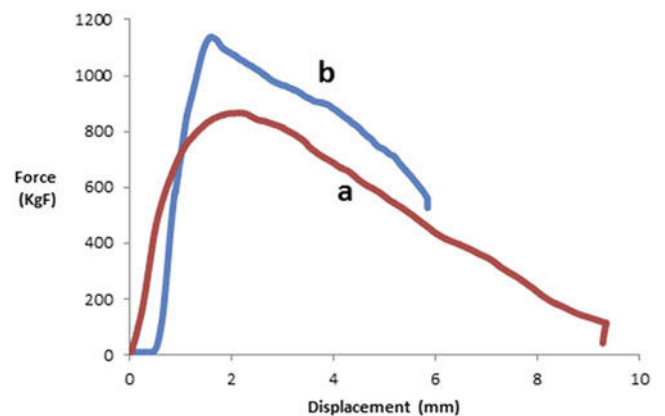


FIG. 9. Load–displacement curves obtained from push-out tests on (a) AlCoat and (b) CuCoat bimetals.

possess very high hardness which may increase the potential for embrittlement of the joint.<sup>26,31</sup> Hence, to avoid the embrittlement and lowering the strength of joint formation of these phases should be avoided to a great extent at the interface.

In the case of CuCoat bimetal, the intermetallic phase thickness at the reaction layer was twice of that in the AlCoat bimetal. Contrary to the expectations, the shear strength of CuCoat bimetal was higher than that of AlCoat which seems to be due to the presence of remaining oxide layer in some regions after aluminizing process. These remaining oxides act as the weak point for initiation of cracks and are responsible for the earlier fracture of AlCoat specimen.<sup>9</sup> Better bonding in CuCoat bimetal can be due to better wettability of Cu with molten aluminum since aluminum cannot wet the aluminum oxides formed on the aluminized steel insert.

#### IV. CONCLUSIONS

The effects of Cu electroplating and aluminizing of steel insert on improving the mechanical strength of Al–Steel bimetal fabricated by compound casting process were investigated. The results are summarized as follows:

(1) The reaction between molten aluminum and steel substrate caused the formation of intermetallic phases ( $\text{Fe}_2\text{Al}_5$  and  $\text{FeAl}_3$ ) at the interface in both bimetals.

(2) Aluminizing and Cu electroplating the steel insert surface as an intermediate layer between solid steel and molten aluminum resulted in optimization of the intermetallic layer thickness as well as improving the metallurgical bonding between the two components.

(3) Silicon and copper are considered as impurity elements in molten aluminum which decrease the activity coefficient of Al atoms in Fe, hence, reducing the thickness of the reaction layer at the interface between the steel insert and Al matrix. However, Si has a more significant effect in this respect.

(4) The thickness of reaction layer in the bimetal Cu-coated insert was twice of that in the bimetal Al-coated insert. Although, the mechanisms for preventing the formation of the intermetallic layer at the interface were different. Cu coating was melted by casting and disappeared, but the aluminide layer remained at the surface of the steel insert and was only partially dissolved in the Al matrix.

(5) The results of push-out tests showed that despite possessing a larger thickness, the interfacial shear strength of the bimetal with Cu-coated insert was higher compared to the one with aluminized insert which was probably due to the presence of remained aluminide oxide layers on the surface of the aluminized steel insert. Better bonding in CuCoat bimetal can be due to better wettability of Cu with molten aluminum since aluminum cannot wet the aluminum oxides formed on the aluminized steel insert.

#### REFERENCES

- J.C. Vaila, M. Peronnet, F. Barbeau, F. Bosselet, and J. Bouix: Interface chemistry in aluminum alloy castings reinforced with iron base insert. *Composites, Part A* **33**, 1417 (2002).
- A. Bouayad, C. Gerometta, M. Radouani, and A. Saka: Interface characterization in aluminum alloy casting reinforced with SG iron insert. *J. Adv. Res. Mech. Eng.* **1**, 226 (2010).
- K.J.M. Papis, B. Hallstedt, J.F. Löffler, and P.J. Uggowitzer: Interface formation in aluminum–aluminum compound casting. *Acta Mater.* **56**, 3036 (2008).
- E. Hajjari, M. Divandari, S.H. Razavi, T. Homma, and S. Kamado: Microstructure characteristics and mechanical properties of Al 413/Mg joint in compound casting process. *Metall. Mater. Trans. A* **43**, 4667 (2012).
- G.R. Zare, M. Divandari, and H. Arabi: Investigation on interface of Al/Cu couples in compound casting. *J. Mater. Sci. Technol.* **29**, 190 (2013).
- E.M. Khoonsari, F. Jalilian, F. Paray, D. Emadi, and R.A.L. Drew: Interaction of 308 stainless steel insert with A319 aluminum casting alloy. *J. Mater. Sci. Technol.* **26**, 833 (2010).
- J. Bruckner: Cold metal transfer has a future joining steel to aluminum. *Weld. J.* **84**, 38 (2005).
- S. Pontevichi, F. Bosselet, F. Barbeau, M. Peronnet, and J.C. Viala: Solid-liquid phase equilibria in the Al–Fe–Si system at 727 °C. *J. Phase Equilib. Diffus.* **25**, 528 (2004).
- E. Aguado, A. Baquedano, U. Uribe, A.I. Fernández-Calvo, and A. Niklas: Comparative study of different interfaces of steel inserts in aluminum castings. *Mater. Sci. Forum* **765**, 711 (2013).
- K.H. Choe, K.S. Park, B.H. Kang, G.S. Cho, K.Y. Kim, K.W. Lee, M.H. Kim, A. Ikenaga, and S. Koroyasu: Study of the interface between steel insert and aluminum casting in EPC. *J. Mater. Sci. Technol.* **24**, 60 (2008).
- B. Lemmens, B. Caklu, J. de Strycker, and K. Verbeken: The effect of Si on the intermetallics formation during hot dip aluminizing. *J. Adv. Mater. Res.* **922**, 429 (2014).
- C.J. Wang and S.M. Chen: The high-temperature oxidation behavior of hot-dipping Al–Si coating on low carbon steel. *Surf. Coat. Technol.* **200**, 6601 (2006).
- F.C. Yin, M.X. Zhao, Y.X. Liu, W. Han, and Z. Li: Effect of Si on growth kinetics of intermetallic compounds during reaction between solid iron and molten aluminum. *Trans. Nonferrous Met. Soc. China* **23**, 556 (2013).
- T.S. Shih and S.H. Tu: Interaction of steel with pure Al, Al–7Si and A356 alloys. *Mater. Sci. Eng., A* **454–455**, 349 (2007).
- W.J. Cheng and C.J. Wang: Microstructural evaluation of intermetallic layer in hot-dipped aluminide mild steel with silicon addition. *Surf. Coat. Technol.* **205**, 4726 (2011).
- U.R. Kattner: *Binary Alloy Phase Diagrams*, 2nd ed. (ASM International, Materials Park, Ohio, 1990).
- G. Ghosh: *Aluminium–iron–silicon, Light Metal Systems: Phase Diagrams, Crystallographic and Thermodynamic Data. Landolt–Börnstein, New Series IV*, Vol. **11A2** (Springer Verlag, Berlin, 2005).
- G. Ghosh: Cost 507. Final Report Group B, The European Commission, 1998.
- G. Ghosh: *Ternary Alloys*, Vol. **5** (VCH publisher, Weinheim, Germany, 1992).
- V.J. Raghavan: Al–Fe–Si aluminum–iron–silicon, section II: Phase diagram evaluations. *J. Phase Equilib. Diffus.* **23**, 362 (2002).
- M.V. Akdeniz and A.O. Mekhrabov: The effect of substitutional impurities on evolution of Fe–Al diffusion layer. *Acta Mater.* **46**, 1185 (1998).
- W. Fragner, B. Zberg, R. Sonnleitner, P.J. Uggowitzer, and J.F. Löffler: Interface reactions of Al and binary Al-alloys on mild steel substrates in controlled atmosphere. *Mater. Sci. Forum* **519–521**, 1157 (2006).
- O. Dezellus, B. Digonnet, and M. Sacerdote-peronnet: Mechanical testing of steel/aluminum-silicon interface by push-out. *Int. J. Adhes. Adhes.* **27**, 417 (2007).
- O. Dezellus, L. Milani, F. Bosselet, M. Sacerdote-Peronnet, and J.C. Viala: Mechanical testing of titanium/aluminum-silicon interface by push out. *J. Mater. Sci.* **43**, 1749 (2008).
- G.H. Awan and F.U. Hasan: The morphology of coating/substrate interface in hot-dip-aluminized steel. *Mater. Sci. Eng., A* **472**, 157 (2008).
- S. Madhavan, M. Kamaraj, and L. Vijayaraghavan: Microstructure and mechanical properties of cold metal transfer welded aluminum/dual phase steel. *Sci. Technol. Weld. Joining* **21**, 194 (2016).
- J.A. Taylor: Iron containing intermetallic phases in Al–Si based casting. *Procedia Mater. Sci.* **1**, 19 (2012).
- L. Backerud, G. Chai, and J. Tamminen: *Solidification Characteristics of Aluminum Alloys. Vol. 2: Foundry Alloys* (AFS/Scanaluminium, Stockholm, Sweden, 1990).



29. C. Wei-Jen and W. Chaur-Jeng: Observation of high-temperature phase transformation in the Si-modified aluminide coating on mild steel using EBSD. *Mater. Charact.* **61**, 467 (2010).
30. H. Springer, A. Kostka, E.J. Payton, D. Raabe, A. Kaysser-Pyzalla, and G. Eggeler: On the formation and growth of intermetallic phases during interdiffusion between low-carbon steel and aluminum alloys. *Acta Mater.* **59**, 1586 (2011).
31. H.R. Shahverdi, M.R. Ghomashchi, S.G. Shabestari, and J. Hejazi: Microstructure analysis of interfacial reaction between molten aluminum and solid iron. *J. Mater. Process. Technol.* **124**, 345 (2002).
32. W. Zhang, D. Sun, L. Han, W. Gao, and X. Qiu: Characterization of intermetallic compound in dissimilar material resistance spot welded joint of high strength steel and aluminum alloy. *ISIJ Int.* **51**, 1870 (2011).
33. L. Backerud, E. Krol, and J. Tamminen: *Solidification Characteristics of Aluminum Alloys. Vol. 1: Wrought Alloys* (Skandaluminium/Universitetsforlaget AS, Stockholm, Sweden, 1986).
34. L. Backerud: Kinetic aspects of the solidification of binary and ternary alloy systems. *Jernkontorets Ann.* **152**, 109 (1968).
35. Q. Wang, X.S. Leng, T.H. Yang, and J.C. Yan: Effect of Fe–Al intermetallic compounds on interfacial bonding of clad material. *Trans. Nonferrous Met. Soc. China* **24**, 279 (2014).